Wind Shear Coefficient at 23 Wind Monitoring Towers in Thailand

Mega Octaviani[1,2], Kasemsan Manomaiphiboon[1,2,*] and Thayukorn Prabamroong[1,2]

[1]The Joint Graduate School of Energy and Environment, King Mongkut's University of Technology Thonburi,
126 Prachautit Rd., Bangmod, Tungkru, Bangkok 10140 Thailand
[2]Center for Energy Technology and Environment, Ministry of Education
*Corresponding author: Tel: +66 2 470 7331, Fax: +66 2 470 733, E-mail: kasemsan_m@jgsee.kmutt.ac.th

Abstract: This study deals with characterization of near-surface wind shear coefficient or exponent using multiple-height wind data observed in the year 2006 at 23 towers located across Thailand. The characteristics of main interest are diurnal and seasonal variations and dependence on atmospheric stability and surface roughness. The key results obtained from the study are: At most towers, wind shear coefficient is relatively large during the night and becomes relatively small in the afternoon, which is typically found or reported in the literature. However, for some towers, the pattern is reverse, which may be partly attributed to complex wind fields influenced by local topography. A set of wind shear coefficient values aggregated from all tower data by type of terrain (open and non-open/rough) and Pasquil-Gifford stability class were analyzed and given, which can be used as a reference for applications in Thailand. It is also evident that the one-seventh power law often used in wind-energy application to extrapolate near-surface wind speed from one height to another is not suitable and wind-energy workers should thus avoid applying it.

Keywords: Wind shear, power law, surface roughness, atmospheric stability, meteorology, wind energy.

1. Introduction

Winds are an alternative and clean energy, which have gained continued interest worldwide. To utilize wind energy, one needs to identify sites or areas with good wind resources. Wind monitoring and numerical modeling generally play a key role in this regard. However, wind monitoring at small or limited heights (e.g., 10-50 m above ground level or agl) is generally not suitable for use to estimate wind power available for wind turbine applications at large heights, and current-day wind turbines can exploit winds at as high as 100-150 m. In case of no wind monitoring available at a large height, extrapolation of wind speed observed at a small height (or small heights) becomes inevitable. One widely used extrapolation method is the wind power law [1] where the ratio of wind speeds at two different heights is given to be proportional to that of the two heights to the power of wind shear coefficient or exponent (α, dimensionless):

$$\frac{v_2}{v_1} = \left(\frac{h_2}{h_1}\right)^{\alpha} . \quad (1)$$

where v_1 and v_2 are the wind speeds at heights h_1 and h_2 (agl), respectively. Rearranging Eq. (1) simply gives

$$\alpha = \frac{\ln(v_2) - \ln(v_1)}{\ln(h_2) - \ln(h_1)} . \quad (2)$$

Here, the term wind shear strictly refers to near-surface (within 10-200 m agl) wind shear, as opposed to upper-level wind shear. The value of 1/7 (~0.143) is often assumed for α when site-specific data is absent, which is called the one-seventh power law. However, it is known that α theoretically varies (i.e., not fixed or constant) with surface roughness length upwind of a wind monitoring site and atmospheric stability [2-4].

Wind shear coefficient has been assessed by many studies. For instance, Farrugia [5] described the seasonal variation of α for the central Mediterranean Island of Malta, with maximum (0.45) in January and minimum (0.29) in July and August, based on wind data at 10 m and 25 m. At the coastal site of Dhulom (Saudi Arabia), Rehman and Al-Abbadi [6] used wind speed data at 20 m, 30 m, and 40 m and found an overall value of 0.255, with the highest value found in October (0.297) and the lowest value in August (0.179). Gualtieri and Secci [4] reported the average values of 0.271, 0.232, and 0.150 at three coastal sites (Brindisi, Portoscuso, and Termini Imerese, respectively) in Southern Italy, based on 6-year wind data at 10-50 m. Schwartz and Elliot [7] used anemometers mounted at larger heights (49-110 m) and found α between 0.18 and 0.28 across sites in the Midwestern US, with relatively low values (0.18-0.20) at the windiest sites.

To our knowledge, the subject of wind shear coefficient has not been much studied in Thailand, particularly considering several sites altogether, which motivated the current study. In fact, this study is a continuation from a preliminary analysis by Manomaiphiboon [8], which investigated α from wind speed data observed at five meteorological towers of the Pollution Control Department (PCD). Two major distinctions of this study from Manomaiphiboon are incorporation of wind data from more towers and a more intensive analysis of wind shear coefficient (here including spatial, diurnal, and seasonal variations and dependence on surface roughness and atmospheric stability). It is hoped that the results or findings obtained from the study will help enhance the existing knowledge related to winds or wind characteristics in the region.

2. Methodology

2.1 Data

Hourly wind data (both speed and direction) in the year 2006 from 23 wind monitoring towers (shortly, towers) were obtained. They belong to the following monitoring networks: the Department of Alternative Energy Development and Efficiency (DEDE) (6 towers: D1-D6), the Electricity Generating Authority of Thailand (EGAT) (12 towers: E1-E12), and the Pollution Control Department (PCD) (5 towers: P1-P5) (Figure 1 and Table 1). The wind data from these towers was also used in a recent wind-resource mapping study for Thailand [9]. The towers are fairly distributed and located in diverse land covers and topographical backgrounds. Table 2 gives a summary of missing and calm-wind (shortly, calm) amounts in the data and monitoring heights by tower. Calm is defined when wind speed is below 0.5 m s^{-1}. Every tower (except E9) has three heights available in monitoring. However, for towers D1-D5 and P1-P5, only two heights were used and their monitoring height of 10 m was excluded as part of our quality assurance. This height is limited and near the surface where wind monitoring could be more easily interfered by nearby natural or man-made objects (e.g., trees and buildings). Such exclusion caused the largest

separation between two consecutive heights to be somewhat limited (e.g., 10 m at D1-D6) and then not ideal in estimating α, which we admit as a limitation of the study. At E1-E8 and E10-E12, data at all available heights were used, and α was computed by averaging individual α values computed from all possible wind pairs, i.e., (20 m and 30 m), (30 m and 45 m), and (20 m and 45 m). Before computing α, any hours with missing or calm values were screened out. Also, any hours with wind directions at two adjacent levels varying greatly (here, >30 degrees in terms of absolute difference or magnitude) were removed, as part of quality assurance. Outliers of wind speed were excluded, and they were here identified as any values smaller than Q1−1.5×IQR or larger than Q3+1.5×IQR, where Q1 is the first quartile, Q3 is the third quartile, and IQR (interquartile range) = Q3−Q1. In descriptive statistics, the first and third quartiles of a sorted dataset correspond to the values below which one-fourth and three-fourth of the data stay, respectively. After the screenings, the remaining data at each tower was found to be ≥75% of the original data, which was considered sufficient for statistical analysis.

2.2 Atmospheric stability

Several methods have been proposed for determining atmospheric stability in the lower part of the atmospheric boundary layer. Here, we considered the classical Pasquill-Gifford (P-G) classification [10-12], by which six atmospheric stability classes are defined: A (strongly unstable), B (moderately unstable), C (slightly unstable), D (neutral), E (slightly stable), and F (moderately-to-strongly stable). The P-G classification is suitable for the current study due to its simplicity while sophisticated classifications, e.g., using Monin-Obukhov length, may not be practical here since they require intensive input parameters or variables in classification. To specify a P-G stability class, we employed the solar radiation/delta-temperature (SRDT) method for a daytime hour and the Turner method for a nighttime hour [12, see Section 6.4 therein]. Both methods are concisely described below. To determine daytime or nighttime hours of a particular day, an algorithm and a computer program to estimate sunrise and sunset times, developed by the National Renewable Energy Laboratory was used [13, http://www.nrel.gov/midc/spa].

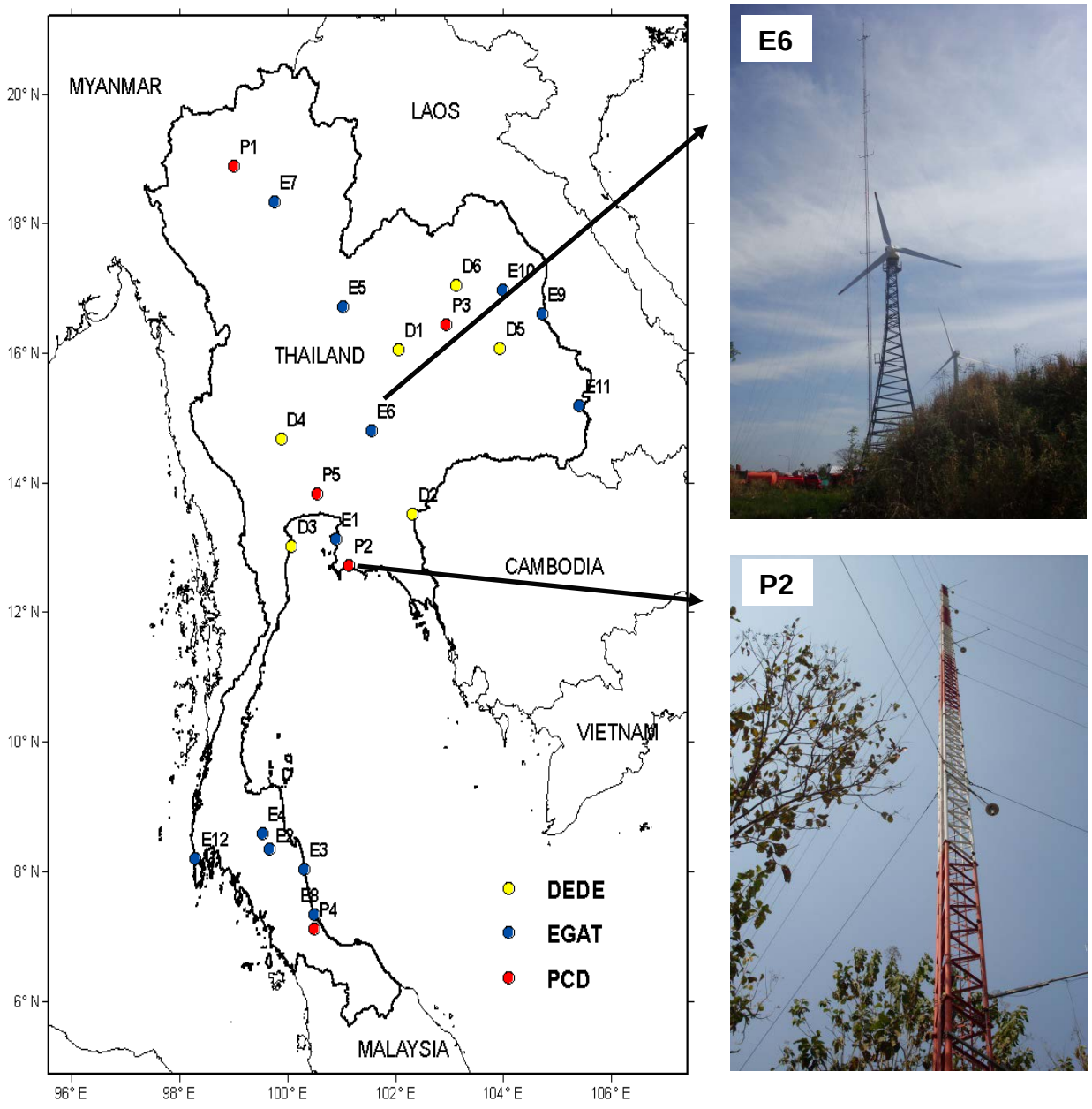

Figure 1. Map of 23 towers. The right-hand-sided panels display the photos of E6 and P2 (taken during 2008-2013 approximately).

Table 1. Towers considered in the study.

Tower[a]	Installation Area	Elevation[b] (m msl)	Site Background[c]
D1	Ban Kao Ya Di, Chaiyaphum	474	On hill/mountain
D2	Ban Khlong Wa, Sakaeo	122	Rural
D3	Ban Laem Pak Bia, Phetchaburi	4	Near coast
D4	Don Chedi, Suphan Buri	30	Rural
D5	Selaphum, Roi Et	144	Rural
D6	Si That, Udon Thani	213	Rural
E1	Ao Pai, Chon Buri	32	On coastal hill
E2	Ban Na, Nakhon Si Thammarat	75	Near hill
E3	Hua Sai, Nakhon Si Thammarat	1	Near coast
E4	Ka Toon, Nakhon Si Thammarat	89	Near reservoir and hill
E5	Khoa Kho, Phetchabun	729	On hill/mountain
E6	Lam Takong Dam, Nakhon Ratchasima	672	On hill top
E7	Mae Moh, Lampang	496	Near valley
E8	Muang Ngam, Songkhla	10	Near coast
E9	Mukdahan, Mukdahan	139	Rural-suburban
E10	Nam Pung Dam, Sakon Nakhon	291	On dam
E11	Sirindhorn Dam, Ubon Ratchathani	148	On dam
E12	Tha Chatchai, Phuket	11	Near coast
P1	Chiang Mai	321	Suburban
P2	Rayong	45	Rural-suburban, near industrial area, near coast
P3	Khon Kaen	152	Rural
P4	Songkhla	6	Near lake
P5	Bangkok	7	Urban

[a] Network: D = DEDE, E = EGAT, and P = PCD
[b] Approximate
[c] Based on visual examination on satellite images (which may not be accurate) or site visit

Table 2. Missings and calms in the available data and mean difference in wind direction.

Tower	Monitoring Height (m agl)	Missing[a] (%)	Calm[a] (%)	Wind Direction Difference (deg.)
D1	30, 40	0.0, 0.0	13.2, 13.5	-[b]
D2	30, 40	0.0, 0.0	12.7, 11.7	-[b]
D3	30, 40	0.0, 0.0	0.2, 0.1	-[b]
D4	30, 40	4.4, 4.4	5.3, 3.3	-[b]
D5	30, 40	0.0, 0.0	4.7, 2.1	-[b]
D6	30, 40	0.0, 0.0	3.2, 4.1	-[b]
E1	20, 30, 45	14.9, 14.9, 14.9	0.3, 1.0, 0.5	4.7[c]
E2	20, 30, 45	0.8, 0.8, 0.8	11.8, 7.7, 6.9	13.8[c]
E3	20, 30, 45	0.4, 0.4, 0.4	1.2, 1.1, 1.3	2.5[c]
E4	20, 30, 45	0.8, 0.8, 0.8	12.0, 12.1, 11.8	14.3[c]
E5	20, 30, 45	0.0, 0.0, 0.0	1.3, 0.5, 0.6	9.8[c]
E6	20, 30, 45	5.2, 5.2, 5.2	0.3, 0.3, 0.4	6.8[c]
E7	20, 30, 45	0.4, 0.4, 0.4	7.9, 10.9, 8.5	7.1[c]
E8	20, 30, 45	0.4, 0.4, 0.4	3.7, 0.7, 0.7	3.7[c]
E9	30, 45	0.0, 0.0	3.7, 2.3	5.3
E10	20, 30, 45	1.2, 1.2, 1.2	7.8, 6.3, 3.6	6.0[c]
E11	20, 30, 45	0.9, 0.9, 0.9	3.9, 2.4, 2.4	4.4[c]
E12	20, 30, 45	0.9, 0.9, 0.9	1.8, 0.9, 2.4	10.4[c]
P1	50, 100	0.6, 1.6	0.0, 0.0	14.2
P2	50, 100	1.4, 2.4	0.1, 0.0	16.2
P3	50, 100	2.0, 3.8	0.3, 0.4	11.4
P4	50, 100	24.4, 26.1	0.0, 0.0	13.1
P5	50, 100	4.3, 6.8	0.3, 0.2	7.8

[a] Values corresponding to the heights in the column of Monitoring Height, respectively
[b] No wind direction data at 40 m available, thus no calculation
[c] No wind direction data at 20 m available

a. SRDT method

For daytime hours, the method uses 10-m wind speed and solar radiation to derive the P-G stability classes. 10-m wind speed was here obtained by the power law. Global solar radiation data was directly observed at P1-P5 but, for the other towers, it was alternatively obtained from the Modern Era Retrospective-analysis for Research and Applications (MERRA) reanalysis data [14]. The MERRA data used here has an hourly resolution, generated with version 5.2.0 of the Goddard Earth Observing System (GEOS) atmospheric model and data assimilation system (DAS) in a grid resolution of 1/2°×2/3°. A bilinear interpolation of the gridded data was made to find solar radiation at a given location.

b. Turner method

For nighttime hours, the method uses 10-m wind speed and cloud cover to determine the P-G stability classes. The method was originally proposed or developed in support of air pollutant dispersion applications [15]. It is noted that due to no cloud cover observations at the towers, they were then estimated from observed cloud cover data from nearby weather stations (within a radius of 60 km from a tower) of the Thai Meteorological Department (TMD) using simple inverse-distance interpolation, and a total of 77 TMD weather stations across Thailand were considered.

2.3 Surface roughness length

The aerodynamic surface roughness length (z_0) varies with type of underlying land cover. Land cover at a particular site may be heterogeneous since more than one land-cover type can be present at or around the site. Here, a procedure suggested in AERSURFACE User's Guide [16] was followed to estimate z_0 for each upwind circular sector at a tower. AERSURFACE is the land/terrain processor in AERMOD, the US EPA's widely used air dispersion modeling system. The procedure is concisely described as follows: First, create a 1-km buffer around a tower and then divide the buffered area into 12×30-degree circular sectors. Next, estimate land cover distribution for each sector using the 2006/2007 land cover data developed by the Land Development Department (LDD) of Thailand [17]. The original LDD data has a scale of 1:25,000, with the UTM (Universal Transverse Mercator) 47N/48N projections in the WGS84 datum. Here, the original LDD land cover data were re-classed to be approximately compatible to the 24-class USGS scheme [18]. The class of urban and built-up land was here further refined into five new urban subclasses according to the extent of building density and height, vegetation intensity, and street widths (see Table 3), based on our visual examination of satellite images [19] and our past site-survey information. Next, assign effective terrain roughness class and length, suggested by Davenport et al. [20] (Table 3). Finally, compute the representative value of $z_{0,rep}$ for each upwind sector as an inverse-distance weighted geometric average:

$$z_{0,rep} = \exp\left(\frac{\sum_{i=1}^{N} d_i^{-1} \ln(z_{0,i})}{\sum_{i=1}^{N} d_i^{-1}}\right), \quad (3)$$

where $z_{0,i}$ is the surface roughness of the i^{th} cell, N is the total number of points or cells within in the circular sector, d_i is the distance between the i^{th} cell and the tower, and ln(.) is the natural logarithm.

3. Results and Discussion

Figure 2 displays the diurnal (i.e., over hours of day) variation of α for each tower. It is seen that α tends to be large during nighttime (7 pm-7 am). This diurnal pattern is in agreement with the findings reported in many studies (e.g., [5-7]) and is closely associated with surface heating/cooling cycle and thus atmospheric stability. Specifically, unstable conditions occur during daytime due to surface heating and then enhance turbulence and smooth the vertical gradient of horizontal wind, resulting in decreased wind shear near the surface. However, such a diurnal pattern is not observed at E5 and E12, where α peaks in the afternoon. This may be partly attributed to vertical wind profiles at these two towers being relatively complex due to the influence of topography for the former but air-sea interaction together with interference by the tree canopy for the latter. Note that E5 is located in a mountainous area while E12 is located at a coastal site surrounded by trees.

Table 3. Surface roughness by land cover.

No.	Description	Roughness Class[a]	Roughness Length (z_0, in m)[a]
1	Urban and built-up land:		
	a. High-rise buildings	8	2.0
	b. High to medium density urban	7	1.0
	c. Medium to low density urban, mixed use of large buildings	5	0.25
	d. Suburban	6	0.5
	e. Semi-rural	4	0.1
2	Dryland cropland and pasture	4	0.1
3	Irrigated cropland and pasture	4	0.1
4	Mixed dryland/irrigated cropland and pasture	4	0.1
5	Cropland/grassland mosaic	4	0.1
6	Cropland/woodland mosaic	5	0.25
7	Grassland	3	0.03
8	Shrubland	3	0.03
9	Mixed shrubland/grassland	3	0.03
10	Savanna	3	0.03
11	Deciduous broadleaf forest	7	1.0
12	Deciduous needleleaf forest	7	1.0
13	Evergreen broadleaf forest	7	1.0
14	Evergreen needleleaf forest	7	1.0
15	Mixed forest	7	1.0
16	Water bodies	1	0.0002
17	Herbaceous wetland	4	0.1
18	Wooded wetland	6	0.5
19	Barren or sparsely vegetated	2	0.005
20	Herbaceous tundra	4	0.1
21	Wooded tundra	4	0.1
22	Mixed tundra	4	0.1
23	Bare ground tundra	3	0.03
24	Snow or ice	2	0.005

[a] Davenport et al. [20]

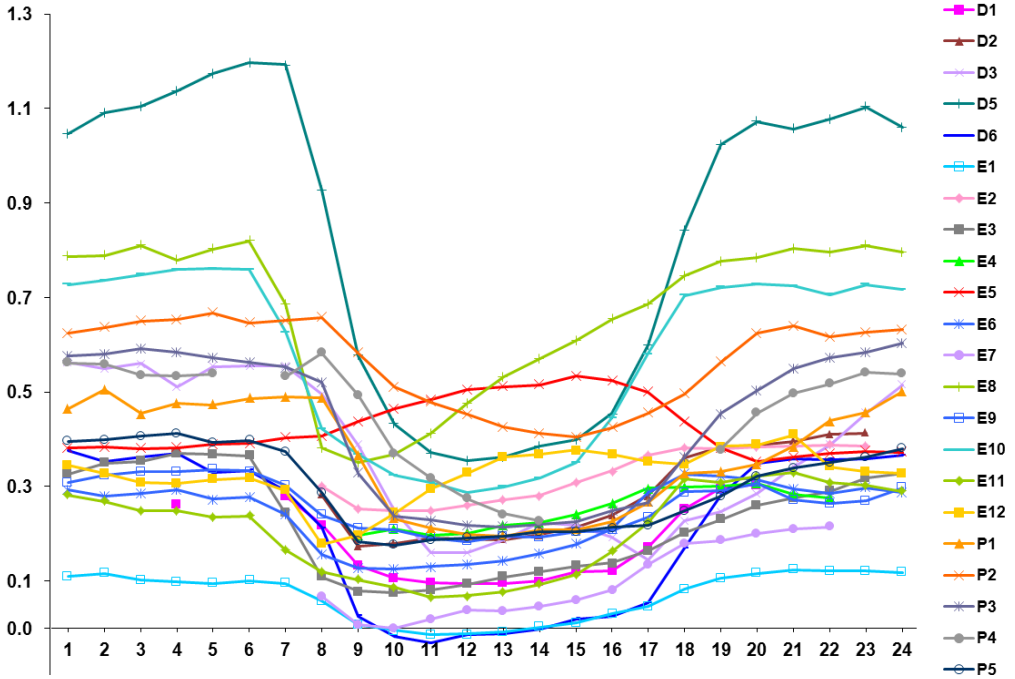

Figure 2. Diurnal variation of wind shear coefficient by tower.

Table 4 presents seasonal (here, 3-monthly) average α: (1) December-February (DJF), (2) March-May (MAM), (3) June-August (JJA), and (4) September-November (SON). As seen, most values (87% of all seasonal cases) are larger than 1/7 and more than half (55%) doubles this value. The degree of seasonal variation generally appears to be less than that of diurnal variation, i.e., α does not greatly differ from its annual average (ANN). The largest annual average is 0.81 at D5 while the smallest is 0.07 at E1. As seen, there is no consistent or common seasonal pattern of α found among all towers. Nevertheless, α is largest in JJA at 11 towers and smallest in MAM at 9 towers.

Table 4. Seasonal and annual averages of wind shear coefficient by tower.

Tower	α				
	DJF	MAM	JJA	SON	ANN
D1	0.15	0.21	0.22	0.24	0.21
D2	0.34	0.29	0.32	NA	0.31
D3	0.35	0.28	0.46	0.33	0.36
D4	0.69	0.52	0.60	0.80	0.64
D5	0.70	0.86	0.81	0.90	0.81
D6	0.24	0.11	0.18	0.28	0.20
E1	0.08	0.08	0.04	NA	0.07
E2	0.36	0.34	0.32	0.33	0.34
E3	0.21	0.19	0.26	0.22	0.22
E4	0.28	0.19	0.20	0.27	0.24
E5	0.29	0.47	0.67	0.27	0.43
E6	0.20	0.20	0.37	0.21	0.24
E7	0.11	0.12	0.15	0.12	0.13
E8	0.73	0.67	0.53	0.74	0.67
E9	0.21	0.31	0.30	0.23	0.26
E10	0.50	0.55	0.60	0.59	0.56
E11	0.29	0.19	0.13	0.22	0.20
E12	0.25	0.30	0.42	0.32	0.32
P1	0.36	0.32	0.36	0.40	0.36
P2	0.58	0.62	0.62	0.42	0.56
P3	0.42	0.43	0.46	0.40	0.43
P4	NA	0.40	0.46	NA	0.43
P5	0.29	0.26	0.34	0.28	0.29

NA: Not available (i.e., not computed) due to less than 70% of total valid records

The dependence of α on P-G stability class and terrain type is shown in Table 5. Each α value in the table is the average of α values from all towers in the same case (i.e., same terrain type under same stability class). As seen, α ranges between 0.18-0.59. In both open terrain ($z_0 \leq 0.1$) and non-open/rough terrain ($z_0 > 0.1$), α decreases from class A to class C and then tends to increase towards class F. α also increases as z_0 increases under the unstable classes (A-C) but decreases under near-neutral and stable conditions (D-F). Theoretically, the one-seventh power law is only appropriate for wind profiles over a smooth terrain up to the first 100 m under near-neutral conditions [21] but our results does not apply, i.e., α being larger than 1/7 (here 0.32 and 0.28 for open terrain and non-open/rough terrain, respectively). In comparison between the values for the open terrain found here and those suggested for a rural area in the literature [12, see Table 6.2 therein], the values found here tend to be about 4 times larger in classes A and B but appear to be close or comparable in classes E and F. It is of additional interest to look back to Figure 2 where α becomes largest at D5 (among all towers) during nighttime hours, and the reason of this is that the terrain background at D5 is rural, open, and relatively smooth with a relatively large number of class-F occurrences. On the contrary, α is relatively small (<0.1) at E1, especially in the nighttime, which is possibly attributed to that E1 is located on a coastal hill and winds at the tower are relatively complex due to topography and air-sea interaction, and that class F does not occur dominantly as in the previous case of D5.

Table 5. Aggregated wind shear coefficient (average ± standard deviation) by P-G stability class and surface roughness.

P-G Stability Class	α (averaged over all valid records and all towers)	
	Open Terrain ($z_0 \leq 0.1$ m)	Non-Open/Rough Terrain ($z_0 > 0.1$ m)
A (strongly unstable)	0.32 ± 0.32	0.38 ± 0.29
B (moderately unstable)	0.31 ± 0.33	0.32 ± 0.27
C (slightly unstable)	0.18 ± 0.18	0.21 ± 0.17
D (neutral)	0.32 ± 0.32	0.28 ± 0.28
E (slightly stable)	0.31 ± 0.20	0.30 ± 0.19
F (moderately-to-strongly stable)	0.59 ± 0.39	0.52 ± 0.33

In summary, wind shear coefficient over Thailand was characterized using multiple-height wind data observed in 2006 at 23 tower locations. Several methods and tools were employed in the study, e.g., surface meteorological data, reanalysis data, local land cover data, stability determination, and satellite imagery examination. Two limitations of the study that should be noted are 1) the separation of wind measurement heights is not much at many towers and 2) due to the nature of the meteorological variables available to and used in the study, atmospheric stability was determined using only the simple methods (i.e., SRDT and Turners). As for the key findings obtained from the study, they are as follows:

- The diurnal pattern of wind shear coefficient shows relatively large values during the night and relatively small values during the day (particularly, in the afternoon) at most towers, which is typically expected. However, the pattern becomes reverse at some sites, which may be partly attributed to complex wind fields influenced by local topography, which is subject to further investigation.
- The aggregated values of α (Table 5) by terrain type and P-G stability class can be useful for wind-energy applications in the region and may also be of interest to wind-energy workers in comparing wind shear coefficient from different regions.
- Lastly, the one-seventh power law generally does not hold for Thailand. All aggregated values of α (Table 5) were found to be larger than 1/7, and thus applying this law directly may potentially lead to substantial underestimation of wind power potential that is linearly proportional to cubed wind speed.

Acknowledgements

The authors gratefully acknowledge contributions from the Department of Alternative Energy Development and Efficiency, the Electricity Generating Authority of Thailand, and the Pollution Control Department for the availability of tower data, the Thai Meteorological Department for the surface meteorological data, and the Land Development Department for the land cover data. The authors received general assistance from the JGSEE Computational Laboratory (Bang Khun Thian Campus). This work was financially supported by the JGSEE, the Thailand Research Fund (under Grant No. RDG5050016), the Electricity Generating Authority of Thailand (under Grant No. 56-B104000-109-IO.SS03A3008178-KMUTT), and the National Science and Technology Development Agency and the Electricity Generating Authority of Thailand (under Grant No. P-12-00858).

References

[1] Manwell JF, McGowan JG, Rogers AL, *Wind energy explained: Theory, design and application* (2002) John Wiley & Sons, New York.

[2] Irwin JS, A theoretical variation of the wind profile power law exponent as a function of surface roughness length and stability, *Atmos Environ* 13 (1979) 191-194.
[3] Bailey BH, Predicting vertical wind profiles as a function of time of the day and surface wind speed, *Proceedings of an international colloquium on wind energy* (1981) Brighton, UK.
[4] Gualtieri G, Secci S, Wind shear cofficients, roughness length and energy yield over coastal locations in Southern Italy, *Renew Energy* 36 (2011) 1081-1094.
[5] Farrugia RN, The wind shear exponent in a Mediterranean island climate, *Renew Energy* 28 (2003) 647-653.
[6] Rehman S, Al-Abbadi NM, Wind shear coefficient, turbulence intensity and wind power potential assessment for Dhulom, Saudi Arabia, *Renew Energy* 33 (2008) 2653-2660.
[7] Schwartz M, Elliot D, Towards a wind energy climatology at advanced turbine hub-heights, *Preprint of the 15th AMS Conference on Applied Climatology* (2005) Savannah, GA.
[8] Manomaiphiboon K, Investigation of wind shear characteristics at five 100-m meteorological towers in Thailand, *Proceedings of the 5th Eco-Energy and Materials Science and Engineering Symposium* (2007) Pattaya, Thailand.
[9] Manomaiphiboon K, Prabamroong, A, Chanaprasert, W, Rajpreeja, N, Phan TT, *Wind resource assessment using advanced atmospheric modeling and GIS analysis* (2010) Final Report, supported by Thailand Research Fund.
[10] Pasquill F, The Estimation of the dispersion of windborne material, *Meteorol Mag* 90 (1961) 33-49.
[11] Gifford FA, Use of routine meteorological observations for estimating atmospheric dispersion, *Nuclear Safety* 2 (1961) 47-57.
[12] Environmental Protection Agency (EPA), *Meteorological monitoring guidance for regulatory modeling applications* (2000) EPA-454/R-99-005, Office of Air Quality Planning and Standards, Research Triangle Park, NC, Available online: http://www.epa.gov/scram001/guidance/met/mmgrma.pdf.
[13] Reda I, Andreas A, *Solar Position Algorithm for Solar Radiation Applications, NREL Report No. TP-560-3430* (2008) 55pp, Colorado. Available online: http://www.nrel.gov/docs/fy08osti/34302.pdf.
[14] Rienecker MM, Suarez MJ, Gelaro R, Todling R, Bacmeister J, Liu E, Bosilovich MG, Schubert SD, Takacs L, Kim GK, Bloom S, Chen J, Collins D, Conaty A, da Silva A, et al., MERRA - NASA's Modern-Era Retrospective Analysis for Research and Applications, *J Climate* 24 (2011) 3624-3648.
[15] Turner DB, A diffusion model for an urban area, *J Appl Meteor* 3 (1964) 83-91
[16] US Environmental Protection Agency (US EPA), *AERSURFACE User's Guide* (2008) Office of Air Quality Planning and Standards, Research Triangle Park, NC. Available online: http://www.epa.gov/scram001/7thconf/aermod/aersurface_userguide.pdf.
[17] Land Development Department (Ministry of Agriculture and Cooperatives), *Land Use and Land Cover Data for Thailand for the Years 2006-2007* (2007) [CD-ROM].
[18] Anderson JR, Hardy EE, Roach JT, Witmer RE, A land use and land cover classification system for use with remote sensor data, *U.S. Geological Survey Professional Paper 964* (1976) U.S. Government Printing Office, Washington, D.C. Available online: http://landcover.usgs.gov/pdf/anderson.pdf.
[19] Google, *Google Earth* (Version 6.0.3.2197) [Software]. Mountain View, CA. Available online: http://earth.google.com.
[20] Davenport AG, Grimmond CSB, Oke TR, Wieringa J, Estimating the roughness of cities and sheltered country, *Preprint of the 12th AMS Conference on Applied Climatology* (2000) 96-99, Asheville, NC.
[21] Panofsky HA, Dutton JA, *Atmospheric turbulence: models and methods for engineering applications* (1984) John Wiley, New York.

